International Journal of Hydrogen Energy 55 (2024) 164–176

Contents lists available at ScienceDirect

International Journal of Hydrogen Energy

journal homepage: www.elsevier.com/locate/he

Zero-cost partial decarbonization of natural gas via molten salt pyrolysis

Schalk Cloete [a,*], Florine Melone [b], Carlos Arnaiz del Pozo [c], Chaitanya Dhoke [a], Øistein Farmen [d], Abdelghafour Zaabout [e]

[a] Process Technology Department, SINTEF Industry, Trondheim, Norway
[b] Génie Chimique, Toulouse INP-ENSIACET, Toulouse, France
[c] Departamento de Ingeniería Energética, Universidad de Politécnica de Madrid, Madrid, Spain
[d] Department of Energy and Process Engineering, Norwegian University of Science and Technology, Trondheim, Norway
[e] Applied Chemistry & Engineering Research Center of Excellence, University Mohammed 6 Polytechnic, Ben Guerir, Morocco

ARTICLE INFO

Handling Editor: Ramazan Solmaz

Keywords:
Natural gas pyrolysis
Molten salt pyrolysis
Techno-economic assessment
Hydrogen
Carbon
Decarbonization

ABSTRACT

Partial decarbonization of natural gas has the potential to kickstart the hydrogen economy. Up to 20% hydrogen volume can be safely accommodated in existing natural gas networks, removing the problem of insufficient distribution and end-use infrastructure for pure hydrogen. The present work investigates a technological pathway for producing such partially decarbonized gas (PDG) at zero or negative cost: molten salt pyrolysis. When producing PDG with 20% H_2 instead of pure hydrogen, the demands on the pyrolysis process become considerably lighter: The pyrolysis reactor can be operated at lower temperatures, alleviating challenges with salt evaporation and reactor corrosion, there is no need for a hydrogen purification step, and the smaller quantities of carbon produced from pyrolysis will not rapidly oversaturate high-value carbon markets. Techno-economic assessments showed that the pyrolysis pathway can produce PDG at a CO_2 avoidance cost of only 11 €/ton compared to 135 €/ton for conventional autothermal reforming. When the reactor temperature is increased from 800 °C to 900 °C or additional natural gas preheating is done, the CO_2 avoidance cost can fall to about −50 €/ton, making PDG production profitable even without climate policies. This promising economic performance combined with the alleviation of multiple technical and political barriers highlights the strong commercial potential of PDG production via molten salt pyrolysis.

1. Introduction

The global clean energy transition has gathered strong momentum in recent years. However, real-world outcomes continue to deviate widely from the net-zero emission pathways regularly published by prominent institutions such as the IEA [1] and the IPCC [2]. These deviations are gradually forcing the world to acknowledge various practical decarbonization realities. Arguably the three most important of these are 1) a mere tenth of the projected peak global population has thus far crossed the 1000 $/month income threshold [3] that would barely qualify as decent living standards by Western norms, 2) popular green energy solutions have limited reach outside the 20% of global final energy consumption served by electricity [1], and 3) material [4] and land-use constraints [5] are already imposing considerable constraints at the current minor shares of modern green energy. The practical implications of these realities are that energy demand growth, especially in the form of heavy industry, machinery, and transportation required to lift billions out of poverty, will continue and that green electricity production has limited scope to abate these emissions. This is among the reasons why global CO_2 emissions keep rising despite the momentum and policy support behind clean energy, most prominently wind and solar power. As a result, the projected emissions overshoot by 2030 relative to a 1.5 °C emissions pathway is 23–27 $GtCO_{2,eq}$/year [6] (half of total global greenhouse gas emissions).

Given the above constraints, practically realistic energy transition pathways must allow for the continued dominant role of energy-dense fuels in the global energy system and accept that economic upliftment outweighs climate change as a priority for a large majority of global citizens. Thus, practical and economical decarbonization of fuels must be a central objective. Hydrogen is often considered as the primary candidate for this vital role. However, hydrogen faces multiple serious challenges, primarily a lack of transmission and end-use infrastructure, a low volumetric energy density that makes it much less practical than traditional fuels, and high production and distribution costs.

The present study explores a technological pathway to partially

* Corresponding author. Flow Technology Group, SINTEF Industry, S.P. Andersens vei 15B, 7031, Trondheim, Norway.
E-mail address: schalk.cloete@sintef.no (S. Cloete).

https://doi.org/10.1016/j.ijhydene.2023.11.124
Received 1 September 2023; Received in revised form 18 October 2023; Accepted 10 November 2023
Available online 22 November 2023

Nomenclature

Acronyms

4C	Counter-current carbon cleaner
CAC	CO_2 avoidance cost
CCS	CO_2 Capture and Storage
IEA	International Energy Agency
IPCC	Intergovernmental Panel on Climate Change
LCOP	Levelized cost of partially decarbonized gas
NG	Natural gas
PDG	Partially decarbonized gas

Symbols

ACF	Annual cash flow (€/year)
C	Annual costs (€/year)
CA	CO_2 avoidance (%)
CAC	CO_2 avoidance cost (€/ton)
CONG	Cost of natural gas (€/GJ)
E	CO_2 emissions intensity (ton/GJ)
i	Discount rate (%)
LCOP	Levelized cost of PDG (€/GJ)
LHV	Lower heating value (MJ/kg)
$\dot{m}$	Mass flow rate (kg/s)
NPV	Net present value (€)
n	Plant lifetime + construction time (years)
P	Annual production (GJ/year)
R	Annual revenues (€/year)
t	Year in the plant lifecycle
$\dot{W}_{net}$	Net power production (MW)
η	Efficiency (%)
φ	Capacity factor (%)

Sub- and superscripts

C	Carbon
El	Electric
FOM	Fixed operating and maintenance costs
NG	Natural gas
PDG	Partially decarbonized gas
VOM	Variable operating and maintenance costs

decarbonize natural gas without encountering any of the above-mentioned challenges. It rests on the principle that 15–20% (by volume) of hydrogen can be blended into natural gas pipelines without modifying transmission or end-use infrastructure [7]. This pathway is often considered in proposals to blend pure hydrogen into natural gas networks. Aside from technical challenges related to locally high hydrogen fractions [8], this is a very expensive proposition. Even long-term projections of low-carbon hydrogen production costs [9] are multiple times more expensive than natural gas production (cost curves in the supplementary information of Welsby et al. [10]). In the best-case scenario, advanced H_2 production pathways from natural gas [11,12] more than double the cost of the produced energy relative to the incoming fuel.

A more thermodynamically and economically efficient pathway would be the partial decarbonization of natural gas, purposefully exploiting the milder equilibrium limitations and gas separation requirements compared to pure hydrogen production. Commercially available autothermal reforming (ATR) with pre-combustion CO_2 capture presents a simple solution for such a plant, and it will be assessed as a benchmark technology in the present study. However, another emerging pathway lends itself well to such a partial decarbonization pathway: molten salt pyrolysis.

Research on molten medium (metal or salt) methane pyrolysis has shown a steadily growing interest driven by a multiple of advantages such as the high heat transfer in the melt, but also the potential for better control of the melt composition to manipulate its physical and chemical properties to enhance the reaction kinetics and solid carbon recovery [13–16]. Under relevant operating conditions, methane fed to the melt splits into gaseous hydrogen and solid carbon, the latter depositing in the melt and floating to the surface for easy removal [17]. Research on molten metal focused on mapping out the reaction kinetics by screening different metals, in pure and mixture forms, to improve conversion and lower activation energy [15–18]. The reaction kinetics remain, however slow with high activation energy [17,19], and the recovered carbon has shown high contamination [20]. Molten salt was found to improve carbon purity benefiting from salt solubility in water if a post-product wash is applied. Multiple salt combinations were tested, showing different performances in terms of conversion, carbon purity and structure [13,14,21].

Several techno-economic assessment studies have revealed promising prospects for this process, outperforming existing technologies such as SMR if the reaction kinetics of the process are improved and a market is created to absorb the associated solid carbon product [18,22,23]. Utilizing methane pyrolysis as a pre-reformer targeting only converting the heavier hydrocarbons could create a streamlined, cost-effective technology deployment strategy in existing commercial processes without saturating the solid carbon market [24].

The most important techno-economic concerns facing molten salt pyrolysis are operating challenges from salt evaporation and corrosivity at high temperatures, challenges with removing salt deposits from the pure carbon product, and the limited industrial market for carbon in comparison to the large energy market for decarbonized fuels. These challenges are naturally addressed by lowering the demands on the process when producing partially decarbonized gas (PDG) containing 20% hydrogen by volume instead of pure hydrogen. With this modest natural gas conversion requirement, the reactor temperature can be lowered from 1000 °C to 800 °C, greatly reducing the salt volatility and corrosivity as well as the load on the reactor construction material. Furthermore, converting only a fraction of the incoming natural gas limits the production of pure carbon, allowing a large quantity of PDG to be produced before saturating high-value carbon markets. As an additional benefit, the PDG from pyrolysis will consist almost entirely of CH_4 and H_2 with hardly any of the oxidized species (CO, CO_2, H_2O) present in a PDG from conventional natural gas reforming where oxidants (O_2 or H_2O) are required in the reaction.

To date, no study available in the literature has quantified the economic implications of the above-mentioned benefits. The present work addresses this research gap by conducting a bottom-up techno-economic assessment of a molten salt pyrolysis process producing PDG containing 20% hydrogen. The performance of the pyrolysis process is benchmarked against more conventional pathways relying on autothermal or electrified reforming. Subsequently, pathways to negative-cost PDG production (PDG becoming cheaper than the natural gas feedstock) are explored, and key sensitivities are identified. Finally, the study concludes by outlining the commercial promise of molten salt pyrolysis for PDG production.

2. Methodology

The methodology is presented in four sections: 1) process descriptions of the three main plants assessed, 2) information about process modelling, 3) the economic methodology, and 4) the performance metrics used.

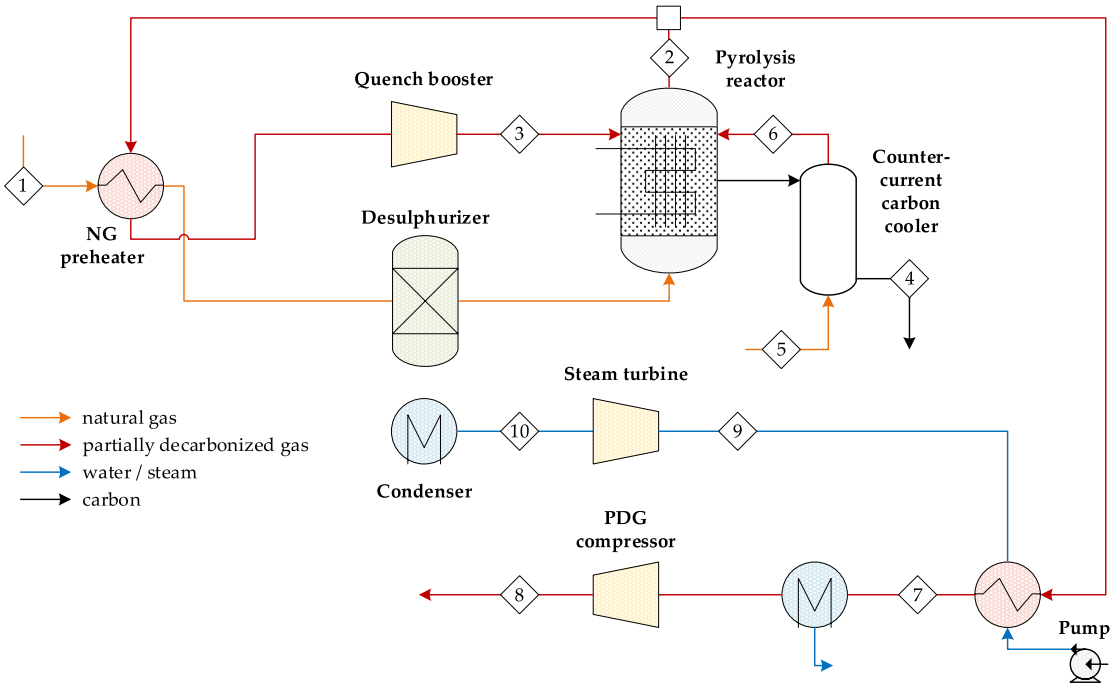

Fig. 1. Process flow diagram of the pyrolysis plant.

Table 1
Stream table of the pyrolysis plant illustrated in Fig. 1.

Stream	m (kg/s)	T (°C)	P (bar)	Mol percentages									
				CH_4	C_2+	H_2	CO	H_2O	CO_2	N_2	O_2	Ar	C
1	73.3	15.0	69.0	89.00	8.11	0.00	0.00	0.00	2.00	0.89	0.00	0.00	0.00
2	88.0	649.5	66.6	76.55	0.02	20.01	0.10	2.51	0.04	0.77	0.00	0.00	0.00
3	20.9	36.9	66.6	76.55	0.02	20.01	0.10	2.51	0.04	0.77	0.00	0.00	0.00
4	10.3	150.0	66.6	0.00	0.00	0.00	0.00	0.00	0.00	0.00	0.00	0.00	100.0
5	4.1	15.0	69.0	89.00	8.11	0.00	0.00	0.00	2.00	0.89	0.00	0.00	0.00
6	3.6	800.0	67.0	76.01	0.02	19.80	0.00	3.27	0.04	0.77	0.00	0.00	0.00
7	66.4	80.0	65.3	76.55	0.02	20.01	0.10	2.51	0.04	0.77	0.00	0.00	0.00
8	64.2	39.3	71.0	78.44	0.02	20.50	0.00	0.10	0.04	0.79	0.00	0.00	0.00
9	42.6	550.0	140.0	0.00	0.00	0.00	0.00	0.00	0.00	0.00	0.00	100.0	0.00
10	42.6	36.0	0.1	0.00	0.00	0.00	0.00	0.00	0.00	0.00	0.00	100.0	0.00

2.1. Process description

This subsection will present the three main plants simulated in this work: the molten salt pyrolysis process and two benchmarks: auto-thermal reforming (ATR) and electrified reforming (ER).

2.1.1. Pyrolysis

The pyrolysis plant simulated in this work is illustrated in Fig. 1 with stream data in Table 1. Natural gas (1) is preheated and desulphurized before being fed to the electrically heated molten salt pyrolysis reactor operated at 800 °C in the base case. To prevent significant quantities of salt from evaporating and fouling downstream equipment, part of the PDG product (2) is recycled, cooled by preheating the incoming natural gas stream, and fed back to the freeboard of the pyrolysis reactor (3). The split of stream 2 is adjusted to achieve sufficient quench to keep the reactor outlet below 650 °C, which should result in manageable levels of evaporated salt entrainment [22]. The carbon product (4) overflows at the top of the reactor and falls through the counter-current carbon cooler where a small quantity of natural gas (5) is fed to cool the carbon and evaporate traces of salt adhered to the carbon product. This natural gas also experiences a small amount of cracking as the carbon itself has some catalytic activity, thus contributing to the PDG production (6). The primary PDG product stream is cooled by raising steam for a steam turbine (9 & 10). After this initial cooling, stream 7 is further cooled, recompressed, and fed back into the natural gas pipeline (8).

2.1.2. Benchmarks

Two benchmark technologies are simulated. The first benchmark is autothermal reforming (ATR), illustrated in Fig. 2 and Table 2. Natural gas (1) is preheated and desulphurized before being mixed with steam (10) raised from the exothermic water-gas shift (WGS) reactions. Higher hydrocarbons are then reformed in the pre-reformer with additional preheating using the hot outlet of the ATR reactor (4). Heat in the ATR is supplied by combusting some of the preheated fuel/steam mixture (2) with oxygen (3) supplied by an air separation unit. The cooled syngas stream (5) is then fed to the high-temperature (HTS) and low-temperature (LTS) shift reactors to convert CO and H_2O into CO_2 and H_2. In addition to raising process steam (10), the heat from the WGS reactions also raises low-pressure steam (9) for solvent regeneration in the MDEA CO_2 capture unit where most of the CO_2 is separated (8) for compression, transport, and storage/utilization. The resulting PDG stream is recompressed and fed back into the natural gas pipeline (7).

The ER benchmark is shown in Fig. 3 and Table 3. Natural gas (1) is preheated and desulphurized before being mixed with process steam

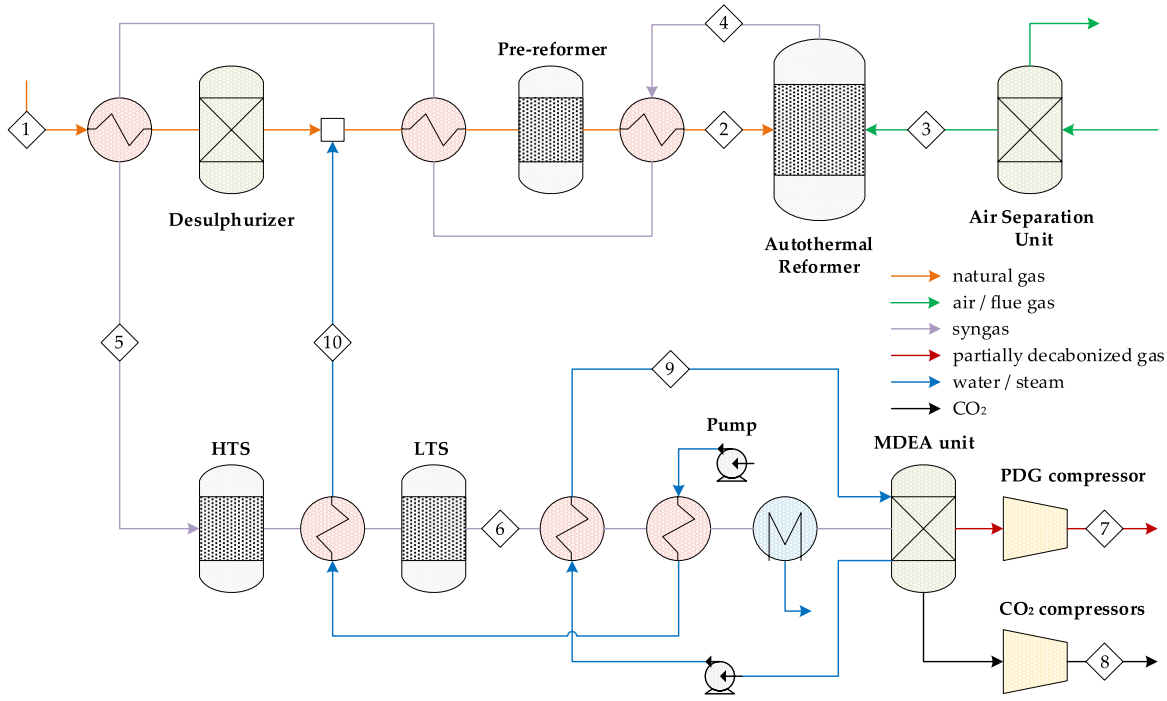

Fig. 2. Process flow diagram of the autothermal reforming (ATR) plant.

Table 2
Stream table of the ATR plant illustrated in Fig. 2.

Stream	m (kg/s)	T (°C)	P (bar)	Mol percentages									
				CH_4	C_2+	H_2	CO	H_2O	CO_2	N_2	O_2	Ar	C
1	6.8	15.0	69.0	89.00	8.11	0.00	0.00	0.00	2.00	0.89	0.00	0.00	0.00
2	17.5	730.0	69.0	39.11	0.00	0.66	0.00	58.78	1.05	0.39	0.00	0.00	0.00
3	6.8	20.3	70.0	0.00	0.00	0.00	0.00	0.00	0.00	1.19	95.01	3.80	0.00
4	24.2	1000.0	69.0	2.25	0.00	44.51	14.83	31.24	6.33	0.37	0.00	0.46	0.00
5	24.2	350.0	69.0	2.25	0.00	44.51	14.83	31.24	6.33	0.37	0.00	0.46	0.00
6	24.2	283.4	69.0	2.25	0.00	58.02	1.33	17.74	19.83	0.37	0.00	0.46	0.00
7	4.5	41.5	70.0	3.55	0.00	91.38	2.10	0.10	1.56	0.59	0.00	0.73	0.00
8	14.2	16.5	100.8	0.00	0.00	0.00	0.00	0.00	100.0	0.00	0.00	0.00	0.00
9	5.4	120.0	1.8	0.00	0.00	0.00	0.00	100.0	0.00	0.00	0.00	0.00	0.00
10	10.7	300.0	69.0	0.00	0.00	0.00	0.00	100.0	0.00	0.00	0.00	0.00	0.00

raised from the WGS reactions (9) and combustion of a fraction of the produced PDG (10). A small amount of PDG combustion in a boiler was required to achieve the steam-to-carbon ratio of 2, assumed as a minimum value needed to avoid carbon deposition in the reformer. The resulting mixture is pre-reformed and further preheated with the hot outlet of the electrified reformer (3). The cooled syngas stream (4) is fed to the WGS reactors and the resulting reaction heat used for raising process steam (9) and low-pressure steam (8) for the MDEA CO_2 capture unit. The MDEA unit separates the CO_2 for compression and storage/utilization (7) and the remaining PDG is recompressed and fed back into the pipeline (6).

2.2. Process modelling

Aspen Plus was used to conduct the process modelling for all plants assessed in this work. Peng-Robinson was used for determining the stream properties. Various other important modelling assumptions are detailed in Table 4.

All reactors were modelled as RGIBBS modules, assuming all reactions proceed to the thermodynamic equilibrium and that the molten salt only acts as a catalyst. Thermodynamic equilibrium is a reasonable assumption for Ni-catalysed reforming reactions, but not for the much slower molten salt pyrolysis reactions. Therefore, the pyrolysis system was simulated not to reach equilibrium conversion by specifying the RGIBBS reactor at a lower temperature and adding a process heater afterward to ensure that the PDG product exits at the reactor temperature. The equilibrium temperature in the pyrolysis RGIBBS module (always below the actual reactor temperature) was adjusted to achieve the specified H_2 fraction in the PDG (20% by volume in the base case). Subsequently, the difference between the simulated conversion and equilibrium conversion at the reactor temperature is used to calculate the required gas residence time in the reactor (and thereby the reactor size) according to the methodology outlined in greater detail in a previous work [25].

Specifically, the reactor height (H) [m] in Eq. (1) is adjusted so that the outlet CH_4 molar concentration ($C_{CH_4,out}$) [mol/m^3] equals the simulated value from the RGIBBS reactor operated at a temperature below the actual reactor temperature, where $C_{CH_4,in}$ is the inlet CH_4 concentration and $C_{CH_4,eq}$ is the equilibrium concentration at the real reactor temperature. Bubble column parameters including the void fraction of small ($\epsilon_{s,b}$) and large ($\epsilon_{l,b}$) bubbles and the rise velocity of small ($U_{s,b}$) and large ($U_{l,b}$) bubbles [m/s] were estimated from the correlations of Wilkenson et al. [27]. The temperature-dependent reaction rate constant (k) [1/s] was derived from a small-scale molten salt

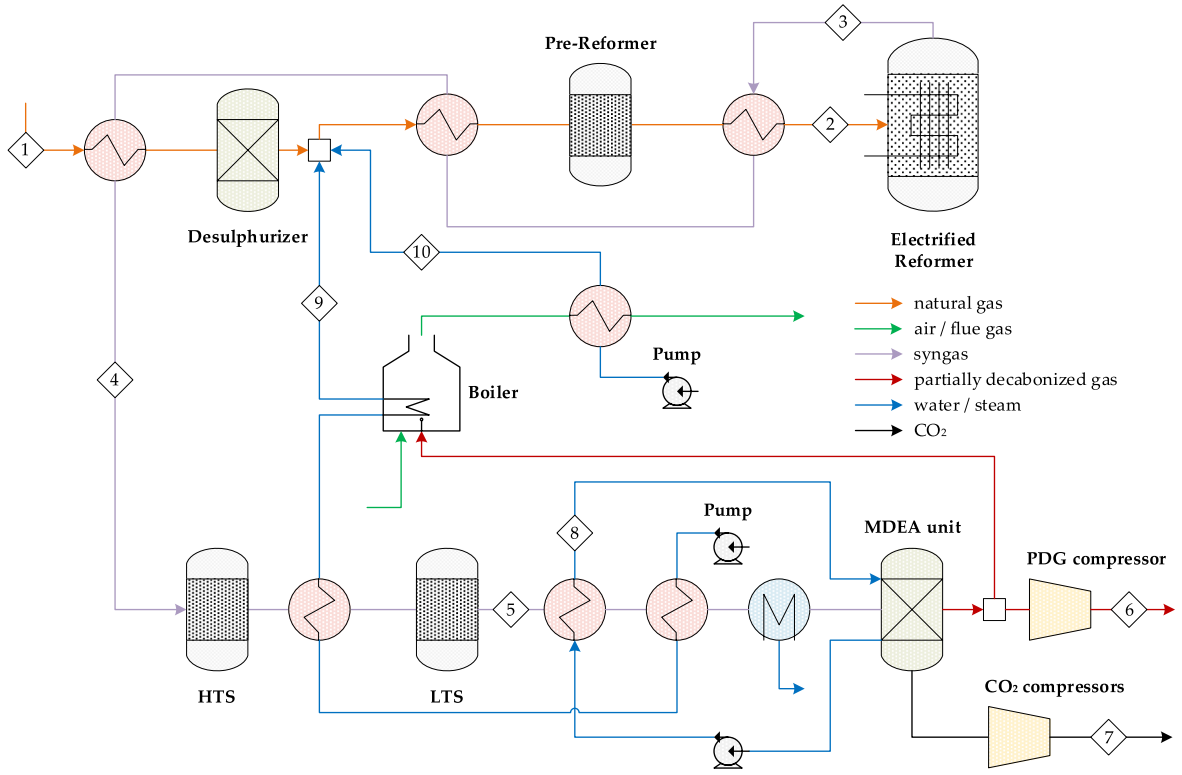

Fig. 3. Process flow diagram of the electrified reforming (ER) plant.

Table 3
Process flow diagram of the ER plant illustrated in Fig. 3.

Stream	m (kg/s)	T (°C)	P (bar)	Mol percentages									
				CH_4	C_2+	H_2	CO	H_2O	CO_2	N_2	O_2	Ar	C
1	6.1	15.0	69.0	89.00	8.11	0.00	0.00	0.00	2.00	0.89	0.00	0.00	0.00
2	18.9	920.0	69.0	30.92	0.00	4.91	0.02	61.90	1.93	0.32	0.00	0.00	0.00
3	18.9	1000.0	69.0	4.89	0.00	53.93	13.75	23.55	3.66	0.22	0.00	0.00	0.00
4	18.9	394.9	69.0	4.89	0.00	53.93	13.75	23.55	3.66	0.22	0.00	0.00	0.00
5	18.9	275.2	69.0	4.89	0.00	66.06	1.62	11.42	15.79	0.22	0.00	0.00	0.00
6	4.5	41.5	70.0	6.64	0.00	89.71	2.20	0.09	1.07	0.30	0.00	0.00	0.00
7	10.7	16.5	100.8	0.00	0.00	0.00	0.00	0.00	100.0	0.00	0.00	0.00	0.00
8	4.2	120.0	1.8	0.00	0.00	0.00	0.00	100.0	0.00	0.00	0.00	0.00	0.00
9	10.5	500.0	69.0	0.00	0.00	0.00	0.00	100.0	0.00	0.00	0.00	0.00	0.00
10	2.4	500.0	69.0	0.00	0.00	0.00	0.00	100.0	0.00	0.00	0.00	0.00	0.00

pyrolysis reactor operated with different catalytically active $KCl/MnCl_2$ salt mixtures [26]. Thus, the methodology can be interpreted as a scale-up of experimental results observed in the laboratory.

$$C_{CH_4,out} = C_{CH_4,eq} + \frac{\epsilon_{s,b}\exp\left(-\frac{k}{U_{s,b}}H + ln\left(C_{CH_4,in} - C_{CH_4,eq}\right)\right) + \epsilon_{l,b}\exp\left(-\frac{k}{U_{l,b}}H + \ln\left(C_{CH_4,in} - C_{CH_4,eq}\right)\right)}{\epsilon_{s,b} + \epsilon_{l,b}} \quad \text{Eq. 1}$$

Since the kinetic model employed only accounts for methane (the most difficult hydrocarbon component to crack), the contribution of higher hydrocarbons introduces some uncertainty. The methodology employed here assumes that the higher hydrocarbons would crack rapidly in a manner that leaves the methane mol fraction in the incoming natural gas approximately unchanged at 89%. Based on experiments showing that propane cracks into approximately equal parts of CH_4 and H_2 (with a stoichiometric balance of C) and achieves complete conversion within a short residence time [28], this should be a reasonable assumption.

2.3. Economic assessment

The economic assessment was carried out using the standardized economic assessment (SEA) tool developed by the authors [29] (a user's guide is available online [30]). This tool assesses standard process units such as compressors, heat exchangers, and vessels with cost correlations from Turton et al. [31], whereas capacity-cost correlations were used for other process units based on cost data from Spallina et al. [32], Shuster

Table 4
Key assumptions implemented in the process simulations.

Parameters	Values	Units
H_2 production rate in PDG	2	kg/s
Compressor isentropic efficiency	85	%
Compressor mechanical efficiency	95	%
Turbine isentropic efficiency	85	%
Turbine Mechanical efficiency	95	%
Minimum approach in heat exchangers	10	°C
Pressure drop in heat exchangers (gas)	2	% of inlet stream
Pressure drop in heat exchangers (liquid)	0.4	bar
Cooling tower water inlet temperature	40	°C
Cooling tower water outlet temperature	20	°C
NG and PDG delivery (pipeline) pressures	69	bar
Natural gas inlet temperature	15	°C
ATR outlet temperature	1000	°C
ER outlet temperature	1000	°C
Pyrolysis reactor temperature	800–900	°C
ASU energy demand	343.4	kWh/tonO_2
Steam turbine inlet temperature	550	°C
Steam turbine inlet pressure	140	bar
Steam turbine outlet pressure	0.05	bar
Excess air flow rate in the boiler	1.1 times	Stoichiometric requirement

Table 5
Economic evaluation assumptions.

Capital estimation methodology		
Bare Erected Cost (BEC)		SEA Tool Estimate
Engineering Procurement and Construction (EPC)		10% of BEC
Process contingency (PS) – applied to the pyrolysis reactor		30% of BEC
Project Contingency (PC)		20% of (BEC + EPC + PS)
Total Plant Cost (TPC)		BEC + EPC + PS + PC
Owner's Costs (OC)		15% of TPC
Total Overnight Costs (TOC)		TPC + OC
Operating & maintenance costs		
Fixed		
Maintenance	2.5	%TOC
Insurance	1	%TOC
Labour	60	k€/y/person
Operators	20	Persons
Variable		
Natural gas	6.5	€/GJ
Electricity	60	€/MWh
Process water	6	€/ton
Make-up water	0.35	€/ton
CO_2 tax	100	€/ton
CO_2 T&S cost	20	€/ton
Salt make-up	2	€/kg
Salt lifetime	2	years
Carbon sales price[a]	500	€/ton
Cash flow analysis assumptions		
1st year capacity factor	65	%
Remaining years	85	%
Discount Rate	8	%
Construction period	2	years
Plant Lifetime	25	years

[a] Implemented as a negative cost.

et al. [33], Liu et al. [34], and Arnaiz del Pozo et al. [35]. The complete SEA tool spreadsheets with all calculations are available online.[1]

The pyrolysis reactor was represented by two process vessels: an inner shell constructed from a Ni-alloy to carry the thermal and corrosion loads and a carbon steel shell outside a 20 cm insulation layer to carry the pressure load. The cost of the inner vessel was increased by 50% to account of additional reactor-specific elements like gas distributors and a carbon removal mechanism. Electrical heating elements in the pyrolysis reactor and the electrified reformer are represented as heating wires and a transformer based on costs from Stack et al. [36].

Once the bare erected cost of each unit in the plant is determined using the above methods, it is scaled for currency, year, and location to 2020 Euros in Western Europe. Additional multipliers are then added to determine the total overnight cost as described in Table 5. Subsequently, fuel and other operating costs as well as revenues from carbon sales are calculated according to the assumptions detailed in Table 5 and a cash flow analysis is completed to determine the levelized cost of the PDG product (see the subsequent section for more details).

2.4. Performance metrics

Various efficiency metrics are defined to characterize the performance of the plants evaluated in the present study. In general, plants consume natural gas and some electricity to produce PDG and, in the case of pyrolysis, carbon. Thus, PDG, carbon, and electric efficiencies are defined according to Eq. (2) - Eq. (4), noting that the electric efficiency is negative when power is consumed. The overall efficiency (Eq. (5)) is taken simply as the sum of the three individual efficiencies.

$$\eta_{PDG} = \frac{\dot{m}_{PDG} LHV_{PDG}}{\dot{m}_{NG} LHV_{NG}} \quad \text{Eq. 2}$$

$$\eta_{C} = \frac{\dot{m}_{C} LHV_{C}}{\dot{m}_{NG} LHV_{NG}} \quad \text{Eq. 3}$$

$$\eta_{El} = \frac{\dot{W}_{net}}{\dot{m}_{NG} LHV_{NG}} \quad \text{Eq. 4}$$

$$\eta = \eta_{PDG} + \eta_{C} + \eta_{El} \quad \text{Eq. 5}$$

CO_2 avoidance is calculated by comparing the CO_2 emissions intensity (ton/GJ) of the produced PDG to that of natural gas. These emissions intensities are determined by fully combusting these respective streams in the flowsheet (isothermally under ambient conditions) to determine how much CO_2 is released per unit of heat produced. No CO_2 emissions are associated with electricity consumption, inherently assuming that the electricity is either carbon-free or any CO_2 emissions are already priced into the electricity cost used in the economic assessment. Similarly, the carbon is assumed to be consumed in an end-use application where it will not be oxidized and emitted as additional CO_2.

$$CA = \frac{E_{NG} - E_{PDG}}{E_{NG}} \quad \text{Eq. 6}$$

In terms of economic performance, the key indicators are the levelized cost of PDG (LCOP) and the CO_2 avoidance cost (CAC). The LCOP is determined by performing a cash flow analysis based on the assumptions detailed in Table 5. The LCOP is the selling price of PDG required to set the net present value (NPV) of the plant to zero.

$$NPV = \sum_{t=0}^{n} \frac{ACF_t}{(1+i)^t} \quad \text{Eq. 7}$$

$$ACF_t = \varphi \cdot (R_{PDG} + R_C - C_{NG} - C_{VOM}) - C_{capital} - C_{FOM} \quad \text{Eq. 8}$$

$$R_{PDG} = LCOP \bullet P_{PDG} \quad \text{Eq. 9}$$

The CAC is subsequently calculated based on the LCOP, the cost of the natural gas (CONG) it displaces, and the CO_2 emissions intensities of the two fuels.

$$CAC = \frac{LCOP - CONG}{E_{NG} - E_{PDG}} \quad \text{Eq. 10}$$

[1] https://bit.ly/44VLWgE.

3. Results and discussion

Results will be presented and discussed in five sections: 1) benchmarking of partial natural gas decarbonization via pyrolysis against more conventional autothermal reforming (ATR) and electrified reforming (ER) routes, 2) the effect of carbon cleaning technology, 3) the effect of reactor operating temperature and H_2 product fraction, 4) the potential offered by more advanced preheating schemes, and 5) the sensitivity to six uncertain parameters.

3.1. Benchmarking

Fig. 4 shows the comparison of pyrolysis against the ATR and ER benchmarks. The comparison is complicated by the fact that the benchmark technologies performed best when achieving far higher levels of CO_2 avoidance than the 10.7% of the pyrolysis technology delivering a product containing 20% H_2. In other words, the ATR and ER processes generate product streams with much higher H_2 fractions that will release less CO_2 upon combustion. High conversion in these processes was the least-cost option because the relatively large number of process units involved in these processes rapidly increase in cost with the higher natural gas flowrates that must be processed to achieve the targeted H_2 output if the conversion is lowered. Thus, Fig. 4 gives two sets of results: unadjusted results in the top row and adjusted results in the bottom row, where natural gas is added to the product streams of the ATR and ER plants so the blended product achieves identical CO_2 avoidance to pyrolysis.

Under the assumptions employed, the ATR and ER technologies deliver similar levelized costs, albeit with different efficiency and cost breakdowns. Fig. 4 (top-left) shows that ER requires large electricity imports and achieves a thermal efficiency in excess of 100% as electrical energy is converted into chemical potential energy in the electrified reformer. Since electricity is more expensive than natural gas, increasing thermal efficiency at the expense of an equivalent amount of electricity imports is not economically favourable. However, Fig. 4 (top-right) shows that the higher energy costs of the ER plant are compensated by

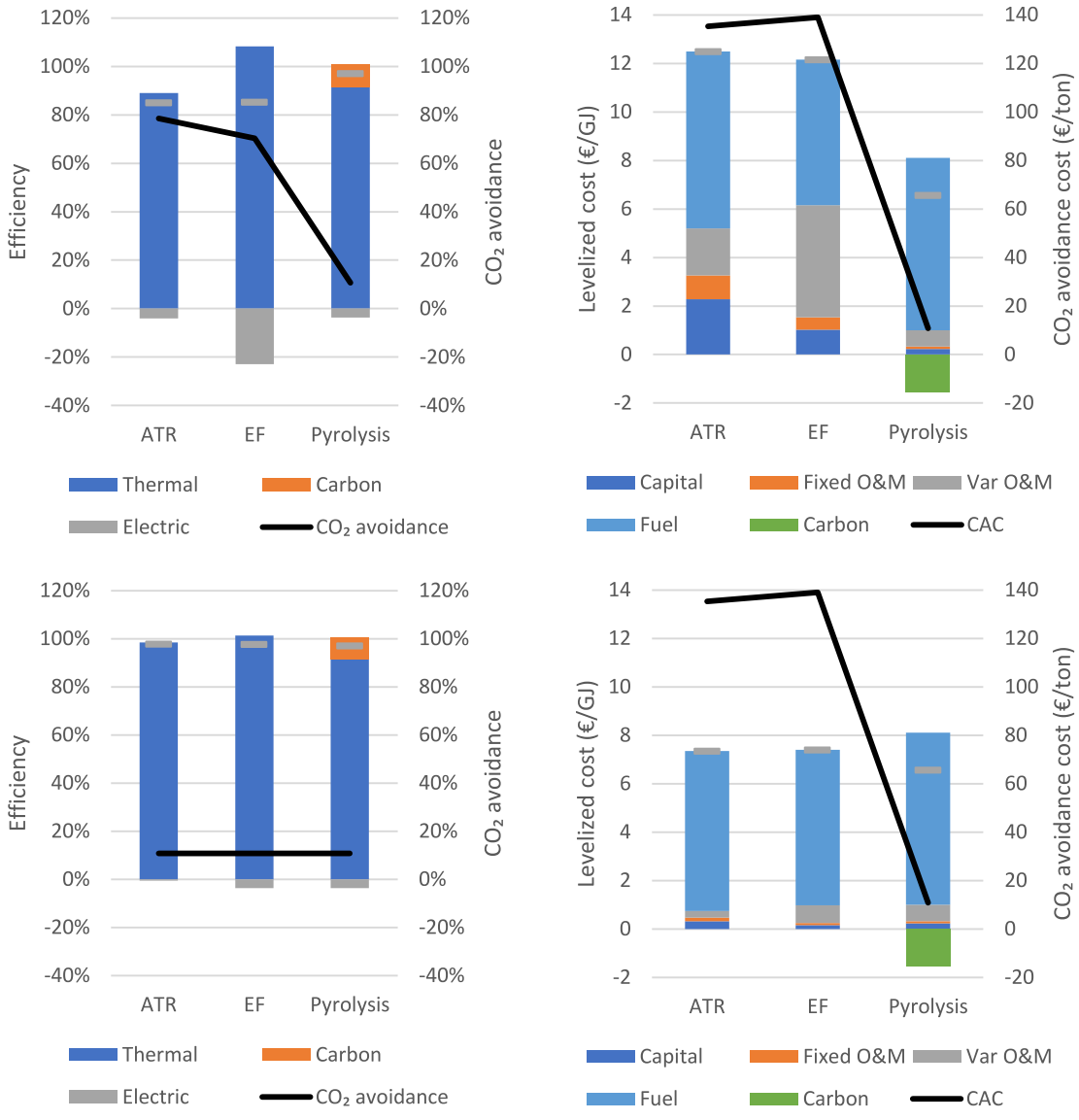

Fig. 4. Benchmarking of pyrolysis targeting 20% H_2 in the product stream at 800 °C reactor temperature against ATR and ER alternatives. Variable O&M costs consist mainly of electricity imports and the grey dashes indicate the summation of the different components of efficiency and levelized cost. Top row: Unadjusted results. Bottom row: Natural gas added to benchmark technologies to yield the same CO_2 intensity as the pyrolysis technology.

lower capital and fixed O&M costs relative to ATR. Capital cost savings originate mainly from avoiding an ASU but also from the electrified reformer costing only about half as much as the autothermal reformer, which includes a high-temperature combustion zone in addition to the reforming zone also present in the electrified reformer. In addition, the ER plant reduces the size of all other units by 10–20% due to a smaller syngas stream with a reduced quantity of oxidized species. Despite these savings, the high cost of consumed electricity and the slightly lower CO_2 avoidance make the ER plant slightly more expensive than the ATR plant in terms of CO_2 avoidance cost.

The pyrolysis technology achieves far lower CO_2 avoidance costs than either benchmark (10.8 €/ton relative to 135.3 €/ton for ATR and 139.0 €/ton for ER). As illustrated in Fig. 4, this large cost advantage is primarily due to revenues from selling pure carbon at 500 €/ton. Without carbon revenues, producing PDG with pyrolysis would be more expensive than the benchmarks, mainly because 9.3% of the incoming natural gas heating value ends up in carbon instead of PDG. Naturally, the economic attractiveness of the pyrolysis pathway will be highly dependent on the carbon price, which will be discussed in a subsequent sensitivity analysis. This carbon product replaces the CO_2 captured for transport and storage from the benchmark plants, which would be a significant practical advantage in regions without access to CO_2 storage/utilization opportunities.

The adjusted efficiencies (Fig. 4, bottom-left) show that the pyrolysis technology consumes as much electricity as the ER case, which is surprising at first glance because methane cracking is much less endothermic than steam methane reforming. This effect results from the limited natural gas preheating done in the base case pyrolysis plant to avoid carbon deposition in the preheater, resulting in more electricity being consumed to heat the large incoming natural gas stream than to drive the endothermic pyrolysis reactions. The economic advantages of further natural gas preheating will be discussed in a later section.

In terms of capital costs, the adjusted numbers (bottom-right in Fig. 4) show that the pyrolysis plant is more capital intensive than the ER plant despite its simplicity. This is due to the relatively high cost of the pyrolysis reactor due to the large volume of unreacted natural gas that must be processed. Still, capital costs (and fixed O&M) are minor cost contributors in these plants that only convert a relatively small fraction of the incoming natural gas stream.

3.2. Carbon cleaning

Fig. 5 shows the small effect of changing the technology for removing traces of salt that will exit with the carbon product. In the authors' prior study focusing on molten salt pyrolysis for pure H_2 production [25], the base case involved carbon washing in hot water. Such an arrangement is relatively costly due to the equipment costs and inefficiency of heat recovery from the carbon stream, the need for large quantities of hot water, and the added cost of the carbon washing vessels.

The present study proposes a more efficient counter-current carbon cleaner (4C) where the carbon falls downward against an upcoming flow of natural gas to evaporate the salt (by presenting an atmosphere with zero salt partial pressure) and cooling the incoming carbon (both via sensible heat transfer and endothermic cracking). The biggest uncertainty related to the 4C arrangement is whether all the salt will be evaporated and carried back into the reactor by the counter-current natural gas stream. The risk of incomplete salt evaporation can be minimized by applying additional microwave heating to heat the carbon in the upper part of the 4C unit to 1200 °C where the salt will evaporate.

As illustrated in Fig. 5 (right), the 4C unit employed in all previous cases significantly reduces the CO_2 avoidance cost relative to conventional carbon washing. This is partly due to lower electricity consumption (0.3 %-points better electric efficiency in Fig. 5, left) resulting from better integration of the heat contained in the carbon and partly due to the avoidance of purified process water required for washing. The addition of microwave heating to ensure complete salt evaporation brings a negligible cost due to the small size of the microwave unit required to increase the carbon temperature by 400 °C and efficient recovery of the additional heat added to the carbon by the counter-current natural gas stream. As an additional benefit, it can also be expected that the 4C system with extra heating will achieve better cleaning results than water washing because even salt traces trapped within a carbon shell will be removed when the salt is evaporated at very high temperatures. Thus, the 4C approach appears to be an attractive pathway for carbon cleaning in molten salt pyrolysis. However, impurity removal is known to be a key challenge for molten media pyrolysis [37], and considerable future work will be required to better understand the techno-economic challenges involved in carbon cleaning.

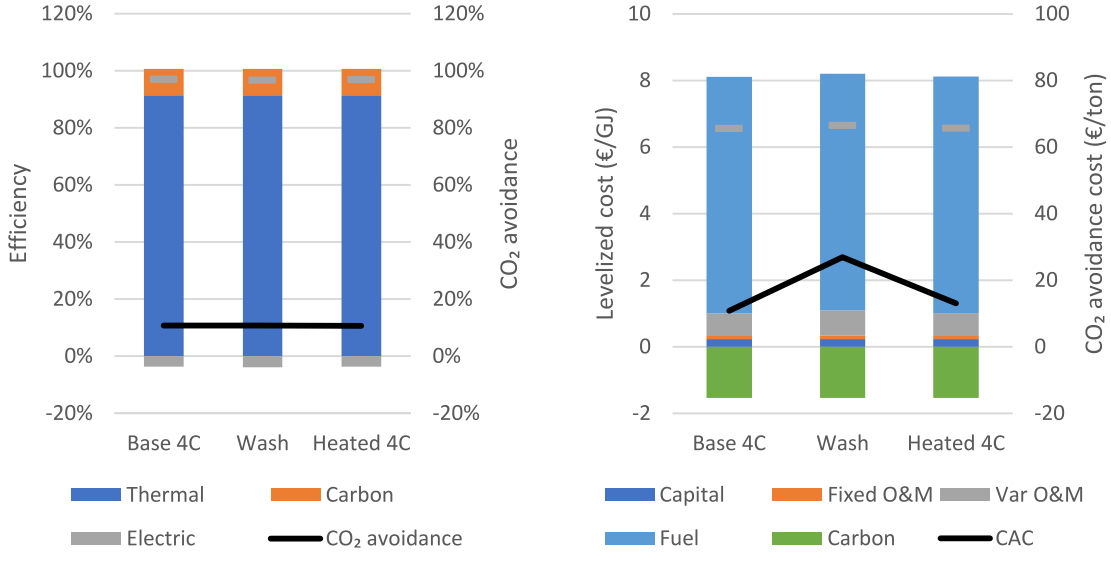

Fig. 5. The effect of carbon cleaning technology on the performance of the pyrolysis technology. 4C = counter-current carbon cleaner.

3.3. Effect of equilibrium approach and operating temperature

High operating temperatures are problematic for molten salt pyrolysis due to salt evaporation and reactor corrosion. Thus, operating at 800 °C instead of 1000 °C will substantially reduce the technological barriers to commercializing molten salt pyrolysis technologies. For example, reactor temperatures of 800 °C reduce the vapour pressure of molten salt by a factor of 15 relative to operation at 1000 °C for the KCl/$MnCl_2$ salt mixture employed here.

Even so, the improved thermodynamics and kinetics offered by higher operating temperatures promise considerable economic benefits if the technical challenges can be overcome. Since the methane cracking reaction is favoured at higher temperatures, higher conversion can be achieved if the temperature is increased. Furthermore, faster kinetics at elevated temperatures significantly reduce the required gas residence time and thus the reactor size. Thus, a specified hydrogen fraction can be achieved with a smaller reactor (lowering capital costs) if the temperature can be increased.

These benefits are illustrated in Fig. 6, where it is clearly illustrated that operation at 900 °C offers significant reductions in the levelized cost and CO_2 avoidance cost relative to operation at 800 °C. It is also noteworthy that the optimal H_2 fraction in the product gas increases from 20% at 800 °C to 40% at 900 °C. Below the optimal point, inefficiencies related to processing large quantities of unreacted natural gas (larger reactor volume to accommodate more gas and increased electricity consumption to heat incoming gas to the reactor temperature) increase the CO_2 avoidance cost. Above the optimal point, a rapid increase in reactor size required to achieve near-equilibrium conversion leads to high costs. For example, the total reactor volume required triples from 20% to 30% H_2 at 800 °C. Elevated temperatures present a more favourable equilibrium that can be approached more closely due to improved kinetics, increasing the optimal H_2 fraction in the PDG product.

Overall, the CO_2 avoidance cost when operating at 900 °C to produce a product gas with 40% H_2 is fully 51.0 €/ton lower than operation at 800 °C to produce a product with 20% H_2. In addition, the CO_2 avoidance cost is negative, reflected in the levelized cost of 6.0 €/GJ for the produced gas, which is well below the 6.5 €/GJ cost assumed for the

Fig. 6. The performance of the pyrolysis technology when delivering different H_2 fractions (higher fractions imply a closer approach to equilibrium requiring larger reactors) at reactor temperatures of 800 and 900 °C.

incoming natural gas. Profitable production of PDG with higher H_2 fractions opens the possibility for greater levels of decarbonization if downstream infrastructure can be improved to safely handle such gas. For perspective, the optimal case at 900 °C increases CO_2 avoidance to 21.4% relative to 10.7% for the optimal case at 800 °C. Alternatively, higher H_2 fractions can be diluted to lower values by mixing with natural gas to stay within safe limits, reducing the CO_2 avoidance of the resulting PDG but keeping the CO_2 avoidance cost unchanged.

3.4. Effect of improved pre-heating

Not having to raise process steam gives methane cracking a significant efficiency advantage over steam methane reforming, but it does present a drawback: limited pre-heating is possible before carbon deposition in the pre-heating heat exchanger becomes a problem. In the present application where only a relatively small fraction of the incoming natural gas is converted, this drawback is enhanced because a large amount of additional electrical energy is required to heat all the unconverted natural gas from the preheating temperature to the reactor temperature. About 40% of this additional electrical energy can be recovered by raising steam from the hot outlet of the pyrolysis reactor, but this brings additional capital costs related to heat exchangers and steam turbines.

It would be much more attractive to recover most of the heat in the reactor outlet stream by pre-heating the incoming natural gas to a higher temperature. Two additional plant layouts were designed to investigate this possibility. The first design assumes that the incoming natural gas is preheated to 630 °C and that the carbon deposition in the preheater can be handled efficiently via cleaning during routine maintenance. Since the heat extracted during preheating is now much larger than the conventional case where the preheating temperature is kept below 300 °C, the entire outlet from the reactor at 650 °C is fed as the hot stream to the preheater (see the "extra preheat" configuration in Fig. 7). After cooling, this stream is split with the required fraction fed back to the reactor freeboard to quench the reactor outlet and the remainder exported as the product gas. The product stream contains some heat, but the temperature is too low for efficient electricity generation so the heat is rejected to cooling water before recompression to pipeline pressures.

The second and most optimistic design also removes the recycle for quenching the reactor outlet (the "max preheat" configuration in Fig. 7). Thus, the outlet stream at 800 °C can be used to preheat the incoming natural gas to 780 °C, almost eliminating the need to use electricity for heating the natural gas. In practice, this case will see even more carbon deposition in the heat exchanger in addition to salt deposition on the other side. To compensate for the high cleaning demands and salt deposition on this heat exchanger, the plant was designed with two

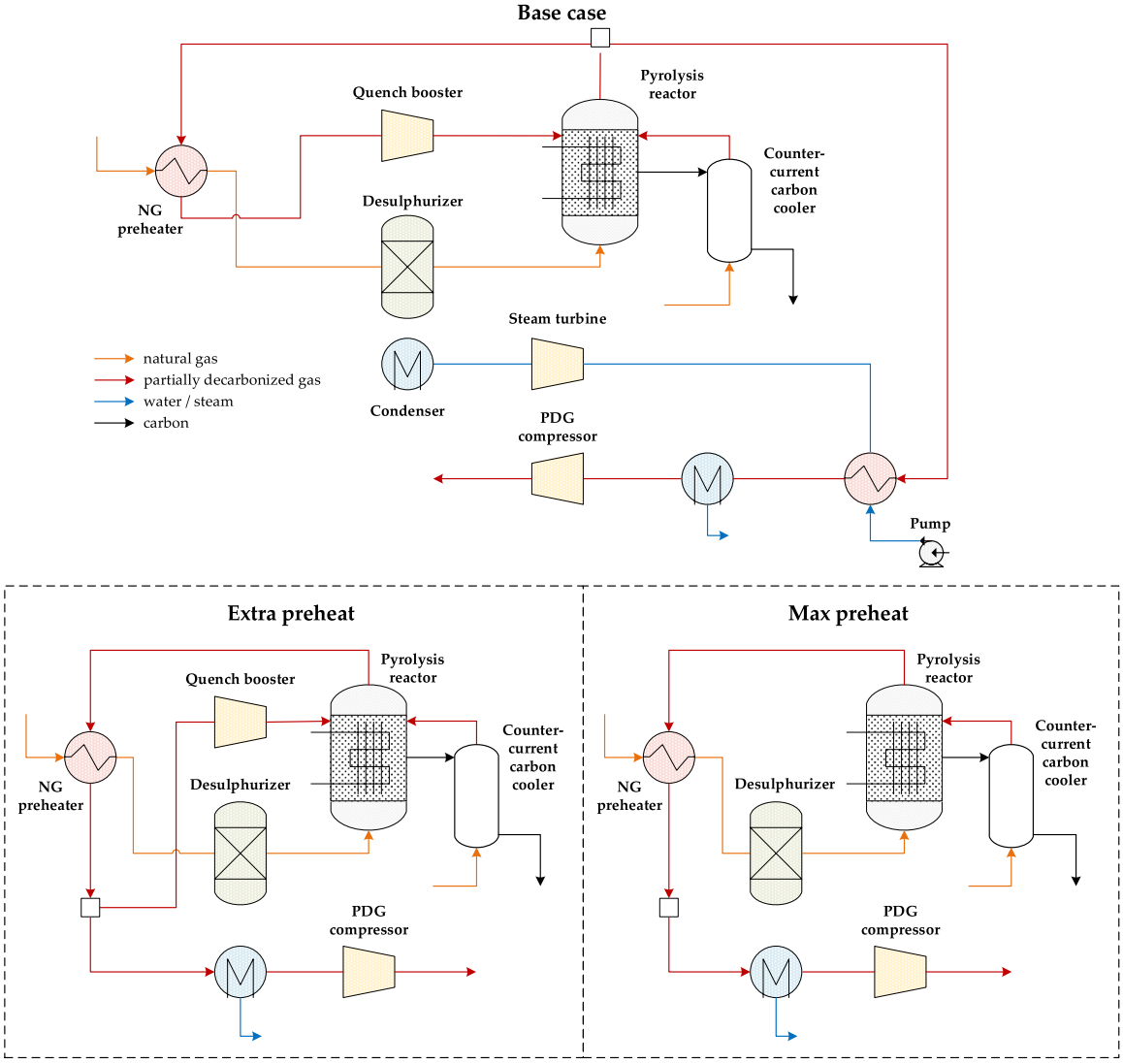

Fig. 7. Illustration of the process simplification enabled by additional preheating.

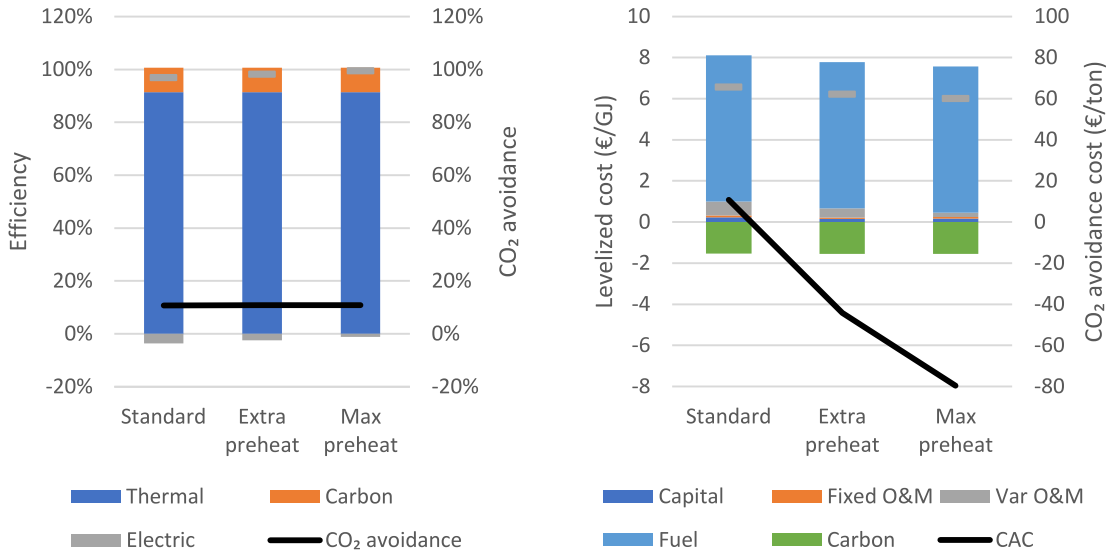

Fig. 8. Effect of increased pre-heating on the performance of the pyrolysis technology delivering 20% H_2 at 800 °C reactor temperature.

parallel preheaters constructed using Ni-alloy instead of stainless steel so that one can always be in operation while the other is being cleaned. Effective heat exchanger design will be essential to enabling this favourable scenario, including mechanisms to remove and recover the deposited carbon and salt.

Fig. 8 shows the large positive effect of additional preheating. In the case with extra preheating to 630 °C, the CO_2 avoidance cost drops from 10.8 to −44.3 €/ton, due to a 34% drop in electricity demand and avoidance of the capital expenditures and O&M costs related to the steam power cycle. Despite the additional parallel heat exchanger in the case with maximum preheating, this case reduced the CO_2 avoidance cost further to −79.7 €/ton by reducing the electricity demand by an additional 35% relative to the base case.

These large economic gains make additional preheating worthy of close investigation before process commercialization. Uncatalyzed carbon deposition at temperatures up to 630 °C may be sufficiently slow to facilitate a reasonable maintenance schedule (e.g., non-catalytic carbon deposition only occurs at practically viable rates above 1200 °C [38]), further helped by the high operating pressure shifting the equilibrium away from carbon formation. Although preheating to 780 °C presents a greater challenge, the additional electricity savings can absorb substantial heat exchanger duplication and cleaning costs. The simplification of the process layout (removing the steam cycle and, in the case with maximum preheating, the quench recycle) also brings significant practical value.

3.5. Sensitivity analysis

The sensitivity of the CO_2 avoidance cost to six influential parameters is shown in Fig. 9. Natural gas price (Fig. 9a) affects the pyrolysis technology the most because it has the lowest thermal efficiency as almost 10% of the incoming fuel heating value is converted to carbon instead of PDG. In contrast, the ER plant derives a small benefit from increased natural gas prices because its thermal efficiency exceeds 100% as electrical energy is converted to chemical potential energy in the electrified reformer (Fig. 4 top-left). The electricity price sensitivity (Fig. 9b) is proportional to the adjusted electric efficiencies (Fig. 4 bottom-left) where the ER and pyrolysis plants present the highest sensitivity. Although not shown, it can be mentioned that the salt cheap, and a doubling of the assumed cost only causes a 1 €/ton increase in the CO_2 avoidance cost.

Naturally, the carbon price (Fig. 9c) has a large impact on the profitability of the pyrolysis plant. If the price falls to 250 €/ton, the CO_2 avoidance cost of pyrolysis reaches the same level as the benchmark technologies. However, pure carbon prices exceeding 500 €/ton are available for high-purity carbon in markets such as anodes, graphite, and activated carbon sorbents. As mentioned in the introduction, the size of these markets is limited, but the relatively small fraction of conversion required to hit the practical limit of 20% H_2 in existing natural gas networks also limits the carbon production to levels that will not rapidly oversaturate these markets. The ATR and ER benchmarks export the removed carbon as CO_2 instead of pure carbon, making them sensitive to the CO_2 transport and storage cost (Fig. 9d). If these conversion processes are built close to oil and gas fields, significant revenues from enhanced oil/gas recovery can be expected, whereas construction in regions without access to good CO_2 storage/utilization opportunities can lead to large costs in this category. However, since natural gas is not highly carbon intensive, the strength of this sensitivity is limited.

Even though Fig. 4 (bottom-right) shows a very small contribution of capital costs, the effects of capital-related uncertainties including the discount rate (Fig. 9e) and scale (Fig. 9f) are significant. The levelized capital costs may be small but so is the level of decarbonization (small denominator in Eq. (10)). The effects of both uncertainties are proportional to the capital intensity of the three plants, with the ATR configuration being the most sensitive, followed by pyrolysis and ER. Even though lower discount rates and larger scales slightly reduce the gap between ATR and pyrolysis, the difference remains very large at the default carbon price of 500 €/ton.

Although no previous studies have investigated molten salt pyrolysis for PDG production, the promising economic prospects of natural gas pyrolysis are confirmed by several studies targeting hydrogen. Depending on assumptions such as the price received for the carbon by-product, prior works agree that pyrolysis can economically outcompete alternative H_2-production pathways [18,23,25,39,40]. Compared to these studies, the promise of the simplified PDG-production plants proposed in the present work is that the product is competitive with unprocessed natural gas, potentially achieving decarbonization at zero or negative costs.

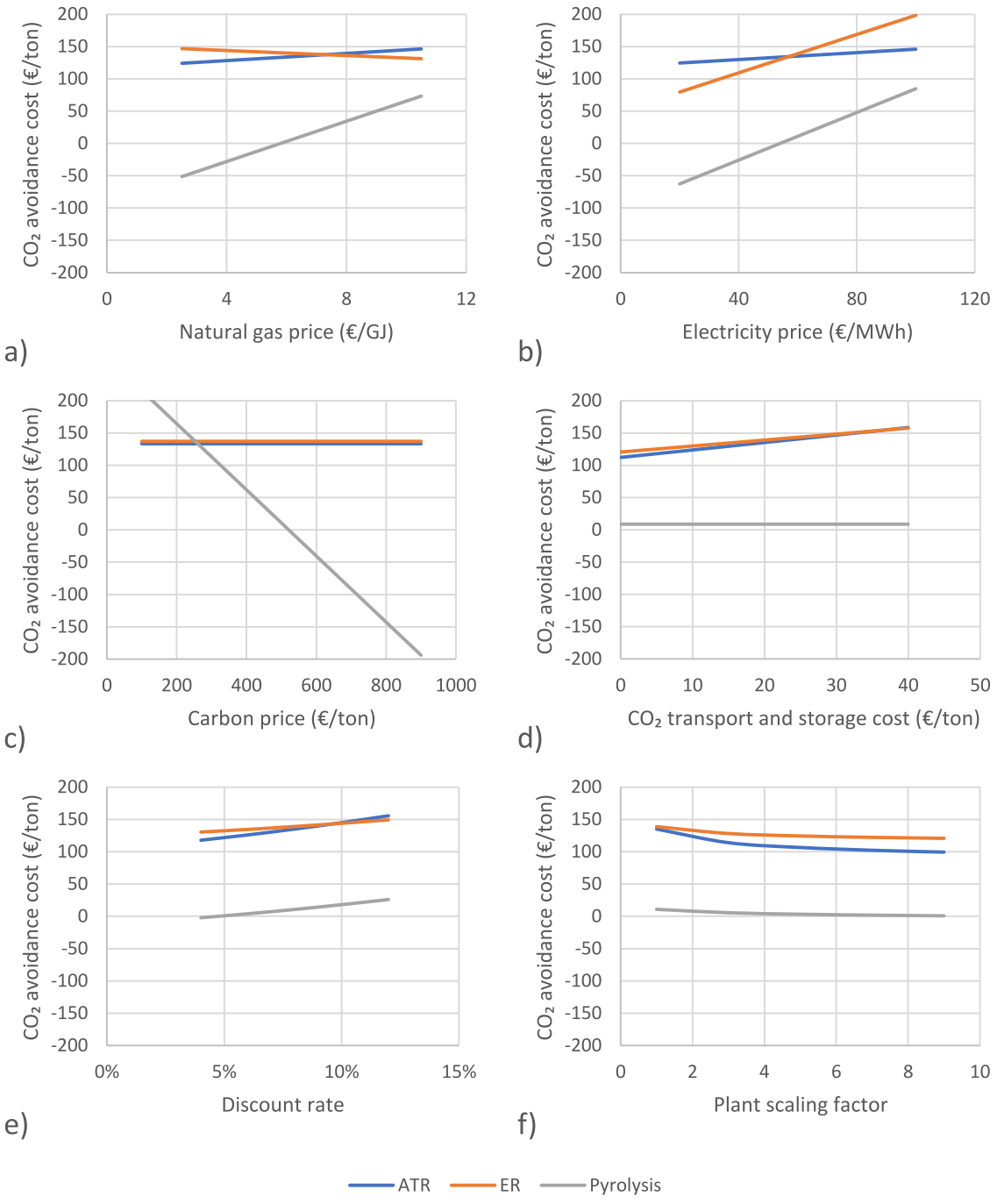

Fig. 9. Sensitivity of the pyrolysis plant delivering 20% H_2 at a reactor temperature of 800 °C and the two benchmark technologies to six influential parameters. The plant scaling factor sets the scale of the present plants equal to 1 and investigates the effect of building larger plants that benefit from greater economies of scale.

4. Conclusions

The present study showed that molten salt pyrolysis holds great promise for producing cost-effective partially decarbonized gas (PDG) that can be accommodated in existing natural gas networks, removing the barrier of insufficient hydrogen infrastructure. The relatively minor conversion also limits the pure carbon output from the process, ensuring that a large quantity of PDG can be produced before high-value carbon markets become oversaturated.

Techno-economic assessment results show that pyrolysis at 800 °C and 70 bar easily outperforms conventional autothermal reforming and electrified reforming routes for PDG production, achieving ~125 €/ton lower CO_2 avoidance costs. The CO_2 avoidance cost of the base case was 10.8 €/ton, but there is clear potential for negative CO_2 avoidance costs. If the reactor can be operated at 900 °C, the CO_2 avoidance cost reduces by 51.0 €/ton and the optimal H_2 fraction in the product increases from 20% to 40%. Similarly, additional preheating of the incoming natural gas stream (which will cause some carbon deposition in the preheater) reduces the CO_2 avoidance cost by 55.1 €/ton. These avenues produce PDG that is cheaper than the incoming natural gas, implying that partial decarbonization via pyrolysis becomes profitable even without the aid of climate policy.

The aforementioned results assume a 500 €/ton selling price for the pure carbon by-product. This assumption represents the main uncertainty in the assessment as every 100 €/ton reduction in carbon selling price increases the CO_2 avoidance cost by 51.2 €/ton. Based on prior carbon market size estimates [25], about 10% of global natural gas production can be profitably converted into PDG by exploiting existing markets for high-purity carbon. Growing demand for high-purity carbon and CO_2 emissions pricing can strongly increase the size of this global market opportunity.

Based on these findings, partial decarbonization of natural gas via molten salt pyrolysis presents a lucrative opportunity for early movers. Accelerated demonstration and scale-up of the moderate-temperature pyrolysis reactor required to realize this opportunity is therefore recommended.

Declaration of competing interest

The authors declare that they have no known competing financial interests or personal relationships that could have appeared to influence the work reported in this paper.

Acknowledgements

This study was supported by the Research Council of Norway under the FRINATEK program (project number: 302819). The pre-submission review by Jan Hendrik Cloete is also gratefully acknowledged.

References

[1] IEA, World Energy Outlook, International Energy Agency, 2022.
[2] IPCC. Climate change 2022: mitigation of climate change. Contribution of working group III to the sixth assessment report of the intergovernmental Panel on climate change. 2022.
[3] Gapminder. Income mountains. 2022. https://www.gapminder.org/fw/income-mountains/.
[4] Kramarz T, Park S, Johnson C. Governing the dark side of renewable energy: a typology of global displacements. Energy Res Social Sci 2021;74:101902. https://doi.org/10.1016/j.erss.2020.101902.
[5] Nøland JK, Auxepaules J, Rousset A, Perney B, Falletti G. Spatial energy density of large-scale electricity generation from power sources worldwide. Sci Rep 2022;12:21280. https://doi.org/10.1038/s41598-022-25341-9.
[6] Cat. Climate action tracker emissions gaps. 2023.
[7] Galyas AB, Kis L, Tihanyi L, Szunyog I, Vadaszi M, Koncz A. Effect of hydrogen blending on the energy capacity of natural gas transmission networks. Int J Hydrogen Energy 2023;48:14795–807. https://doi.org/10.1016/j.ijhydene.2022.12.198.
[8] Eames I, Austin M, Wojcik A. Injection of gaseous hydrogen into a natural gas pipeline. Int J Hydrogen Energy 2022;47:25745–54. https://doi.org/10.1016/j.ijhydene.2022.05.300.
[9] IEA, Global. Hydrogen review 2022. Paris: International Energy Agency; 2022.
[10] Welsby D, Price J, Pye S, Ekins P. Unextractable fossil fuels in a 1.5 °C world. Nature 2021;597:230–4. https://doi.org/10.1038/s41586-021-03821-8.
[11] Nazir SM, Cloete JH, Cloete S, Amini S. Pathways to low-cost clean hydrogen production with gas switching reforming. Int J Hydrogen Energy 2020. https://doi.org/10.1016/j.ijhydene.2020.01.234.
[12] Cloete S, Khan MN, Amini S. Economic assessment of membrane-assisted autothermal reforming for cost effective hydrogen production with CO2 capture. Int J Hydrogen Energy 2019;44:3492–510. https://doi.org/10.1016/j.ijhydene.2018.12.110.
[13] Palmer C, Tarazkar M, Gordon M, Metiu H, McFarland E. Methane pyrolysis in low-cost, alkali-halide molten salts at high temperatures. Sustain Energy Fuels 2021;5:6107–23. https://doi.org/10.1039/d1se01408k.
[14] Kang D, Rahimi N, Gordon M, Metiu H, McFarland E. Catalytic methane pyrolysis in molten MnCl2 -KCl. Appl Catal B Environ 2019;254:659–66. https://doi.org/10.1016/j.apcatb.2019.05.026.
[15] Scheiblehner D, Neuschitzer D, Wibner S, Sprung A, Antrekowitsch H. Hydrogen production by methane pyrolysis in molten binary copper alloys. Int J Hydrogen Energy 2023;48:6233–43. https://doi.org/10.1016/j.ijhydene.2022.08.115.
[16] Msheik M, Rodat S, Abanades S. Experimental comparison of solar methane pyrolysis in gas-phase and molten-tin bubbling tubular reactors. Energy 2022;260. https://doi.org/10.1016/j.energy.2022.124943.
[17] Palmer C, Tarazkar M, Kristoffersen H, Gelinas J, Gordon M, McFarland E, Metiu H. Methane pyrolysis with a molten Cu-Bi alloy catalyst. ACS Catal 2019;9:8337–45. https://doi.org/10.1021/acscatal.9b01833.
[18] Perez B, Jimenez J, Bhardwaj R, Goetheer E, Annaland M, Gallucci F. Methane pyrolysis in a molten gallium bubble column reactor for sustainable hydrogen production: proof of concept & techno-economic assessment. Int J Hydrogen Energy 2021;46:4917–35. https://doi.org/10.1016/j.ijhydene.2020.11.079.
[19] Zeng J, Tarazkar M, Pennebaker T, Gordon M, Metiu H, McFarland E. Catalytic methane pyrolysis with liquid and vapor phase tellurium. ACS Catal 2020;10:8223–30. https://doi.org/10.1021/acscatal.0c00805.
[20] Rahimi N, Kang D, Gelinas J, Menon A, Gordon M, Metiu H, McFarland E. Solid carbon production and recovery from high temperature methane pyrolysis in bubble columns containing molten metals and molten salts. Carbon 2019;151:181–91. https://doi.org/10.1016/j.carbon.2019.05.041.
[21] Kang D, Palmer C, Mannini D, Rahimi N, Gordon M, Metiu H, McFarland E. Catalytic methane pyrolysis in molten alkali chloride salts containing iron. ACS Catal 2020;10:7032–42. https://doi.org/10.1021/acscatal.0c01262.
[22] Pruvost F, Cloete S, Cloete J, Dhoke C, Zaabout A. Techno-Economic assessment of natural gas pyrolysis in molten salts. ENERGY CONVERSION AND MANAGEMENT; 2022. p. 253. https://doi.org/10.1016/j.enconman.2021.115187.
[23] Parkinson B, Matthews J, McConnaughy T, Upham D, McFarland E. Techno-economic analysis of methane pyrolysis in molten metals: decarbonizing natural gas. Chem Eng Technol 2017;40:1022–30. https://doi.org/10.1002/ceat.201600414.
[24] Pruvost F, Cloete S, del Pozo C, Zaabout A. Blue, green, and turquoise pathways for minimizing hydrogen production costs from steam methane reforming with CO2 capture. ENERGY CONVERSION AND MANAGEMENT; 2022. p. 274. https://doi.org/10.1016/j.enconman.2022.116458.
[25] Pruvost F, Cloete S, Hendrik Cloete J, Dhoke C, Zaabout A. Techno-Economic assessment of natural gas pyrolysis in molten salts. Energy Convers Manag 2022;253:115187. https://doi.org/10.1016/j.enconman.2021.115187.
[26] Kang D, Rahimi N, Gordon MJ, Metiu H, McFarland EW. Catalytic methane pyrolysis in molten MnCl2-KCl. Appl Catal B Environ 2019;254:659–66. https://doi.org/10.1016/j.apcatb.2019.05.026.
[27] Wilkinson PM, Spek AP, van Dierendonck LL. Design parameters estimation for scale-up of high-pressure bubble columns. AIChE J 1992;38:544–54. https://doi.org/10.1002/aic.690380408.
[28] Palmer C, Bunyan E, Gelinas J, Gordon MJ, Metiu H, McFarland EW. CO2-Free hydrogen production by catalytic pyrolysis of hydrocarbon feedstocks in molten Ni–Bi. Energy Fuel 2020;34:16073–80. https://doi.org/10.1021/acs.energyfuels.0c03080.
[29] Arnaiz del Pozo C, Cloete S, Álvaro Á Jiménez. Standard economic assessment (SEA) tool. 2021. Available from: https://bit.ly/3IXPWC8.
[30] Arnaiz del Pozo C, Cloete S. Á. Jiménez álvaro, SEA tool user guide. Available from: https://bit.ly/3jq9Bkf; 2021.
[31] Turton R, Bailie RC, Whiting WB, Shaeiwitz JA. Analysis, synthesis and design of chemical processes: appendix A. Pearson Education; 2008.
[32] Spallina V, Pandolfo D, Battistella A, Romano MC, Van Sint Annaland M, Gallucci F. Techno-economic assessment of membrane assisted fluidized bed reactors for pure H2 production with CO2 capture. Energy Convers Manag 2016;120:257–73. https://doi.org/10.1016/j.enconman.2016.04.073.
[33] Shuster E, Goellner JF, Shah V, Turner MJ, Kuehn NJ, Littlefield J, Cooney G, Marriott J. Analysis of natural gas-to-liquid transportation fuels via. Fischer-Tropsch; 2013.
[34] Liu G, Larson ED, Williams RH, Kreutz TG, Guo X. Making Fischer−Tropsch fuels and electricity from coal and biomass: performance and cost analysis. Energy Fuel 2011;25:415–37. https://doi.org/10.1021/ef101184e.
[35] Arnaiz del Pozo C, Álvaro Á Jiménez, Roncal Casano JJ, Cloete S. Exergoeconomic assessment of air separation units for pressurized O2 production incorporating two-phase expanders. Cryogenics 2022;124:103477. https://doi.org/10.1016/j.cryogenics.2022.103477.
[36] Stack DC, Curtis D, Forsberg C. Performance of firebrick resistance-heated energy storage for industrial heat applications and round-trip electricity storage. Appl Energy 2019;242:782–96. https://doi.org/10.1016/j.apenergy.2019.03.100.
[37] Rahimi N, Kang D, Gelinas J, Menon A, Gordon MJ, Metiu H, McFarland EW. Solid carbon production and recovery from high temperature methane pyrolysis in bubble columns containing molten metals and molten salts. Carbon 2019;151:181–91. https://doi.org/10.1016/j.carbon.2019.05.041.
[38] Abbas HF, Wan Daud WMA. Hydrogen production by methane decomposition: a review. Int J Hydrogen Energy 2010;35:1160–90. https://doi.org/10.1016/j.ijhydene.2009.11.036.
[39] Tabat ME, Omoarukhe FO, Güleç F, Adeniyi DE, Mukherjee A, Okoye PU, Ogbaga CC, Epelle EI, Akande O, Okolie JA. Process design, exergy, and economic assessment of a conceptual mobile autothermal methane pyrolysis unit for onsite hydrogen production. Energy Convers Manag 2023;278:116707. https://doi.org/10.1016/j.enconman.2023.116707.
[40] He Y, Song B, Jing X, Zhou Y, Chang H, Yang W, Huang Z. Low-carbon hydrogen production via molten salt methane pyrolysis with chemical looping combustion: emission reduction potential and techno-economic assessment. Fuel Process Technol 2023;247:107778. https://doi.org/10.1016/j.fuproc.2023.107778.